Polymer 50 (2009) 3111–3118

Contents lists available at ScienceDirect

Polymer

journal homepage: www.elsevier.com/locate/polymer

Free-radical propagation and termination kinetics of the butyl acrylate dimer studied by pulsed laser polymerization techniques

Michael Buback [a,1], Thomas Junkers [a,b,*], Matthias Müller [a]

[a] Institut für Physikalische Chemie, Georg-August-Universität Göttingen, Tammannstrasse 6, D-37077 Göttingen, Germany
[b] Preparative Macromolecular Chemistry, Institut für Technische Chemie und Polymerchemie, Universität Karlsruhe (TH)/Karlsruhe Institute of Technology (KIT) Engesserstrasse 18, 76131 Karlsruhe, Germany

ARTICLE INFO

Article history:
Received 3 March 2009
Received in revised form
22 April 2009
Accepted 23 April 2009
Available online 3 May 2009

Keywords:
Acrylates
Kinetics (polym.)
Pulsed laser polymerization

ABSTRACT

The propagation and termination rate coefficients for bulk polymerization of the butyl acrylate dimer (BA dimer) are determined by pulsed laser techniques. The rate coefficient for propagation, k_p, is deduced for temperatures from 20 to 90 °C via the pulsed laser polymerization–size exclusion chromatography (PLP–SEC) method at pulse repetition rates between 1 and 10 Hz. The Arrhenius parameters were found to be: $E_A(k_p) = (34.2 \pm 1.0)$ kJ mol^{-1} and $A(k_p)$/L mol^{-1} s^{-1} $= (1.08 \pm 0.49) \times 10^7$ L mol^{-1} s^{-1}. The termination rate coefficient, k_t, has been measured via SP-PLP–ESR, single pulse-pulsed laser polymerization in conjunction with time-resolved electron spin resonance detection of radical concentration. The resulting Arrhenius parameters as deduced from the temperature range −15 to +30 °C are: $E_A(\langle k_t \rangle) = (22.8 \pm 3.7)$ kJ mol^{-1} and $\log(A/\text{L mol}^{-1}\text{ s}^{-1}) = 10.6 \pm 1$. The chain-length dependence of k_t was studied at 30 °C. For short chains a significant dependence was found which may be represented by an exponent $\alpha = 0.79$ in the power-law expression $k_t(i) = k_t^0 i^{-\alpha}$.

1. Introduction

Since the invention of pulsed-laser polymerization techniques, detailed information on reaction coefficients for free-radical polymerization of most common monomers has been become available [1,2]. Highly accurate rate coefficients of propagation and termination have been collated for styrene [3,4], various acrylates [5–7], methacrylates [5,8–11], itaconates [12,13] and other monomers [5,14,15]. Propagation rate coefficients, k_p, are determined via the IUPAC-recommended pulsed laser polymerization–size exclusion chromatography (PLP–SEC) technique in which k_p is determined from the typical pattern of the molecular weight distribution produced by laser pulsing at constant repetition rate [3]. Termination rate coefficients, k_t, may be accurately obtained by the so-called single pulse-pulsed laser polymerization technique with near-infrared detection of monomer concentration (SP-PLP–NIR) [2,16]. The measured decrease in monomer concentration after applying a single laser pulse is fitted to analytical equations which yields k_t. This method is well suited for rapidly propagating monomers, as monomer conversion per pulse is relatively high. Monomers that propagate at slower rate are more difficult to measure via SP-PLP–NIR, as changes in monomer concentrations are small. This drawback may be avoided by employing single pulse-pulsed laser polymerization carried out in conjunction with electron spin resonance (SP-PLP–ESR) spectroscopy, by which method radical concentrations rather than monomer concentrations are traced [13,17–19].

The simultaneous application of PLP–SEC and SP-PLP–ESR should allow for the measurement of the propagation and termination kinetics even for special types of monomers, such as 1,5-dibutyl 2-methylene pentanedioate, which is the dimer of butyl acrylate (BA dimer) the structure of which is depicted in Scheme 1 together with the structure of the rather similar di-*n*-butyl itaconate (DnBI) monomer.

Studies into the kinetics of the BA dimer are of interest for various reasons: one wants to know whether the propagation and termination rate coefficients are similar to the ones of DnBI (see Scheme 1), which differs from the BA dimer species only in the additional –CH_2– moiety between the two ester functionalities. The rate coefficients for DnBI have already been reported [12,13,20].

Further interest in the BA dimer results from the fact that this monomer constitutes the smallest representative of acrylic macromonomers which are formed upon high-temperature treatment of

* Corresponding author. Institut für Physikalische Chemie, Georg-August-Universität Göttingen, Tammannstrasse 6, D-37077 Göttingen, Germany. Tel.: +49 721 608 2603; fax: +49 721 608 5740.
E-mail addresses: mbuback@gwdg.de (M. Buback), thomas.junkers@polymer.uni-karlsruhe.de (T. Junkers).
[1] Tel.: +49 551 393141; fax: +49 551 393144.

0032-3861/$ – see front matter © 2009 Elsevier Ltd. All rights reserved.
doi:10.1016/j.polymer.2009.04.036

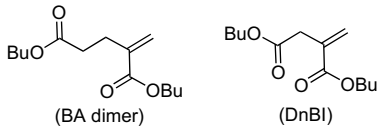

Scheme 1. Structure of the BA dimer (1,5-dibutyl 2-methylene pentanedioate) and di-*n*-butyl itaconate (DnBI).

the corresponding acrylates or via the addition–fragmentation technique [21–23]. The poly(BA dimer) may be looked upon as a polyBA brush where one additional BA unit is located at each ester moiety of the backbone chain as shown in Scheme 2. The polymerization of the BA dimer is thus of interest from both a kinetic perspective and a material science point of view.

The dimer and trimer of methyl acrylate have already been studied [24–26]. Besides their use in addition–fragmentation transfer polymerization, the interest in these monomers results from the fact that the propagating radical mimics the so-called midchain radical (MCR), which may occur in acrylate polymerizations where they are produced by *inter*- and *intra*molecular transfer-to-polymer reactions (for a review on aspects related to the presence of MCRs see [27] and references cited therein). Via such transfer-to-polymer reactions the radical functionality of a secondary propagating acrylate chain-end is transferred onto a carbon atom carrying an ester-moiety. The *intra*molecular transfer preferentially occurs by a 1,5 hydrogen-shift reaction via a six-membered cyclic transition state structure. The driving force behind this 1,5 hydrogen-shift (backbiting) reaction is due to the higher stability of the tertiary MCR as compared to the secondary chain-end radical. The MCRs may undergo monomer addition, although at a much smaller rate than do secondary chain-end radicals, but other reactions, e.g., β-scission processes, may also take place [28]. The understanding of acrylate polymerization kinetics thus requires the rate of monomer addition to the MCR being accurately known, as this reaction converts the tertiary radical back into a rapidly growing secondary radical. Approaches have been developed to determine the monomer addition rate to an MCR via PLP–SEC [29] and via NMR analysis of the resulting (branched) polyBA [30]. Scheme 3 depicts the propagating radicals in BA dimer and DnBI homopolymerization together with the midchain radical occurring in acrylate polymerization. The MCR species and the propagating BA dimer radical are similar to each other with a butyl ester group and a methylene unit sitting next to the radical center. It should be noted that in BA dimer polymerization a bulky BA dimer is added to the chain-end, whereas the midchain radical typically reacts with a considerably smaller BA monomer molecule.

After a brief description of the applied laser techniques, namely the PLP–SEC technique for measuring k_p, and the SP-PLP–ESR technique for measuring k_t, the rate coefficient data obtained at various temperatures will be presented and discussed.

2. Experimental section

2.1. Monomer synthesis

In a Rauhut–Currier reaction (see Scheme 4), 25 g tri-*n*-butyl phosphine were dissolved in 100 ml THF under an inert gas

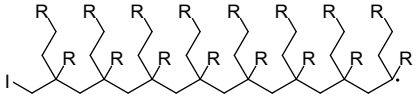

Scheme 2. Propagating radical in BA-dimer polymerization (I stands for an initiator end-group and R for a butyl ester moiety).

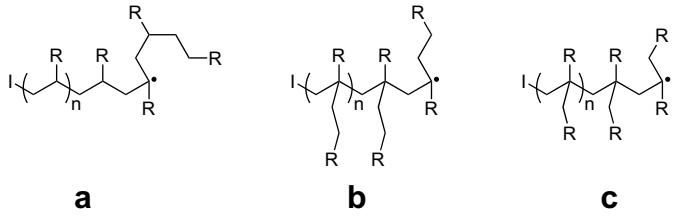

Scheme 3. The midchain radical in (a) BA polymerization and the propagating radicals in (b) BA dimer and (c) DnBI polymerization I is the initiating fragment and R stands for the butyl ester moiety.

atmosphere and brought to 40 °C. 300 ml Butyl acrylate were then added dropwise over a period of 1 h in order to avoid heat build-up due to exothermicity. The temperature stayed below 45 °C during the whole procedure. After addition of all acrylate, the solution was stirred for 15 h. The BA dimer was isolated via distillation at 120 °C/1 torr and no impurities were detected using ^{1}H and ^{13}C NMR.

2.2. Pulsed laser polymerization

Polymerizations were carried out within in a cell consisting of a teflon tube closed by two quartz windows on each side. This cell was placed into an optical high-pressure cell, which was heated using *n*-heptane as the temperature transmitting medium. Monomer conversion was determined spectroscopically with FT-NIR, using an IFS 88 instrument (Bruker), via the absorbance at around 6160 cm^{-1} of the first overtone of the C–H-stretching mode at the C=C double bond [31]. The reaction mixture consisting of monomer and photoinitiator was irradiated by sequences of laser pulses using an LPX 210i excimer laser (Lambda Physik) operated on the XeF-line at 351 nm. Laser pulses were applied at repetition rates, ν_{rep}, between 1 Hz and 10 Hz with the energy per pulse being close to 3 mJ. The photoinitiator, 2,2-dimethoxy-2-phenyl-acetophenone (DMPA, 99%, Sigma–Aldrich) was used as received and employed at a concentration of 0.05 mol L^{-1}. Depending on the particular reaction conditions, between 100 and 1000 pulses were applied to obtain BA dimer conversions between 1.5 and 3.5%. The resulting polymer–monomer mixture was directly subjected to SEC analysis.

2.3. Density measurement

Densities of the initial (BA dimer) bulk polymerization system were determined in the temperature range from 20 to 80 °C with a DMA 60 (Anton Paar) density meter. The instrument was calibrated against air and demineralized water.

2.4. Size exclusion chromatography

Molecular weight distributions were determined at 35 °C by SEC using a Waters 515 pump, a Waters 410 refractive index detector, three PSS-SDV columns with nominal pore sizes of 10^5, 10^3 and 10^2 Å, respectively. Tetrahydrofuran was used as the eluent at a flow rate of 1 mL min^{-1}. Molecular weight calibration was established against narrow polydispersity polystyrene (PS) standards (MW = 410–2 000 000 g mol^{-1}, Polymer Standards Service (PSS) Mainz,

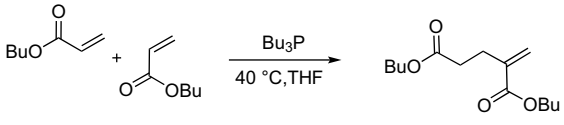

Scheme 4. Rauhut–Currier reaction of butyl acrylate to BA dimer.

Germany). The resulting molecular weight distributions have been recalibrated using Mark–Houwink parameters for poly(BA dimer) ($K = 18.7 \times 10^{-5}$ dL g^{-1}, $a = 0.624$) [32] and for polystyrene ($K = 14.1 \times 10^{-5}$ dL g^{-1} and $a = 0.70$) [33].

2.5. Single pulse-pulsed laser polymerization

The ESR spectra were recorded on a Bruker Elexsys® E 500 series CW-EPR spectrometer. ESR quartz tubes of 5 mm outer and 4 mm inner diameter were fitted into the cavity (resonator). The samples were irradiated through a grid using a COMPex 102 excimer laser (Lambda Physik) operated on the XeF line at 351 nm at a laser energy of about 50 mJ per pulse. The laser beam penetrates the sample tube at right angle to the cylindrical axis. The spectrometer and the laser were triggered via a Scientific Instruments 9314 pulse generator. In between the PLP experiments, the tube was removed from the ESR spectrometer and was inserted into the sample chamber of an IFS 88 FT-NIR spectrometer. The photoinitiator α-methyl-4(methylmercapto)-α-morpholinopropiophenone (MMMP, 98%, Sigma–Aldrich) was used as received at initial concentrations of about 1×10^{-2} mol L^{-1}. The advantage of using MMMP for the SP-PLP–ESR experiments rather than DMPA relates to the fact that photo-dissociation of MMMP yields two primary radicals which both rapidly induce chain growth thus yielding a narrow chain-length distribution of the macroradicals which is a prerequisite for analyzing chain-length-dependent termination [34–36].

3. Results and discussion

3.1. Propagation rate coefficients from pulsed laser polymerization–size exclusion chromatography experiments

The typical shape of a PLP-structured MWD and the associated first-derivative curve are shown in Fig. 1 for a poly(BA dimer) sample produced at 30 °C using a laser pulse repetition rate of 1 Hz. The MWD curve exhibits two distinct components. The first-derivative curve, in addition to the associated $L1$ and $L2$ positions, clearly shows a third point of inflection, $L3$. Each of these three points allows for the calculation of k_p via Eq. (1):

$$L_i = k_p \cdot c_M \cdot t_{0,i} \quad (1)$$

where L_i is the polymer chain length at an inflection point, c_M is the monomer concentration and $t_{0,i}$ the time between the initiating and the terminating laser pulses. For this particular experiment, these time intervals were 1, 2 and 3 s for $L1$–$L3$. As the same k_p is obtained from each specific molecular weight, the information from $L2$ and $L3$ is somewhat redundant. Nevertheless, the overtone positions are highly important, because they serve as an internal consistency criterion. With $L2$ and $L3$ being located at 2($L1$) and 3($L1$), the obtained k_p value are considered as reliable.

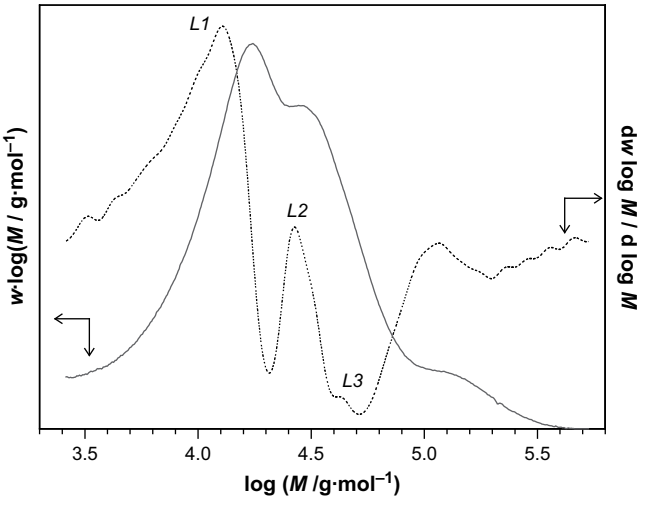

Fig. 1. Molecular weight distribution (solid line) and associated first derivative (dotted line) for poly(BA dimer) from PLP at 1 Hz laser repetition rate and 30 °C.

The entire set of experimental k_p data for the temperature range 20–90 °C is summarized in Table 1. The number of pulses applied to each sample varied from 1700 (at 20 °C) to 60 pulses (at 90 °C). Monomer concentration was calculated from bulk density, which was experimentally found to be:

$$\rho/\mathrm{g\,mL^{-1}} = 0.99966 - 0.00110 \cdot T/^{\circ}\mathrm{C}$$

Pulse laser polymerization was carried out at repetition rates of 1–5 Hz. The determination of k_p should be independent of repetition rate. Variations in k_p with pulse repetition rate may indicate the occurrence of side reactions, such as transfer to polymer in acrylate polymerization [27]. Frequency dependent (apparent) k_p values may also result in case of chain-length-dependent propagation [37–39]. This effect, in general, is relatively small. It should be noted that in case of significant chain-length-dependence of propagation, $k_{p,2}$ should be well below $k_{p,1}$, which is not seen in the present study. The observed slight variation of $k_{p,1}$ with pulse repetition is, however, consistent with the trend expected for $k_p(i)$ decreasing with chain length. Another source of error may result from imperfect characterization of the molecular weight distribution, e.g., due to inaccurate Mark–Houwink (MH) parameters. Although being usually applied to the entire SEC mass range, MH coefficients are only valid for the molar mass range for which they were determined. Especially in the oligomeric short-chain range, where polymers show coiling behavior which differs from the one of large chains, the MH relation may not perfectly hold. For the BA dimer, the MH coefficients were determined via fractionation of a broadly distributed polymer sample followed by MALDI-ToF mass detection to be $K = 18.7$ dL g^{-1} and $a = 0.624$ within the mass range 1100–50 000 g mol^{-1} [32]. Molar masses in Table 1, which were determined beyond this calibration range, are given in italics.

The k_p values derived from the first and second point of inflection are generally in good agreement with each other, as can be seen from the ratio of M_1/M_2 (last column in Table 1), which is mostly fairly close to the theoretical value of 0.5. Deviations are partly due to the molecular weight being outside the calibration range. Shown in Fig. 2 is an Arrhenius plot, which has been constructed from k_p data deduced via $L1$, data for which k_p values from $L1$ and $L2$ differed by more than 10% were not included into the fit. The resulting Arrhenius equation for k_p of the BA dimer reads:

$$\ln\left(k_p/\mathrm{L\,mol^{-1}\,s^{-1}}\right) = 16.20(\pm 0.38) - 4111(\pm 121)\ \mathrm{K}/T \quad (2)$$

The k_p data closely fit to an Arrhenius line. It should be noted that k_p values from experiments at higher temperatures which show no second point of inflection also fit on to the straight line. The Arrhenius straight line behavior up to the highest experimental temperature indicates that the ceiling temperature, where the rate of propagation equals the rate of depropagation, is above the one of DnBI. The latter one has been reported to be around 60 °C, depending on monomer concentration [12].

The Arrhenius Eq. (2) corresponds to an activation energy of (34.2 ± 1.0) kJ mol^{-1} and to a frequency factor of $(1.08 \pm 0.49) \times 10^7$ L mol^{-1} s^{-1}. Thus, as compared to conventional monomers, a relatively large temperature dependence of k_p is found (see discussion with Table 2, further below). The

Table 1
Results from PLP–SEC experiments for the BA dimer.

T/°C	Pulse rate/Hz	c_M/mol L^{-1}	M_1/g mol^{-1}	M_2/g mol^{-1}	$k_{p,1}$/L mol^{-1} s^{-1}	$k_{p,2}$/L mol^{-1} s^{-1}	M_1/M_2
20.8	1	3.81	8240	18480	8.4	9.4	0.45
21	1	3.81	7990	17970	8.2	9.2	0.44
30	1	3.77	12560	25920	13	13.4	0.48
30	3	3.77	4880	10340	15.1	16	0.47
33	1	3.76	17080	33000	17.7	17.1	0.52
35	1	3.75	16780	32670	17.4	17	0.51
40	1	3.73	18890	38250	19.7	20	0.49
40	5	3.73	4540	9690	23.7	25.3	0.47
40	5	3.73	4710	9660	24.6	25.2	0.49
40	5	3.73	4570	9820	23.9	25.7	0.47
40	3	3.73	7180	16030	22.5	25.1	0.45
40.1	1	3.73	18800	37360	19.6	19.5	0.50
49.9	1	3.69	27050	*52080*	28.6	27.5	0.52
50	1	3.69	28220	*51830*	29.8	27.4	0.54
50	5	3.69	6990	15990	36.9	42.3	0.44
50	1	3.69	27260	52910	28.8	28	0.52
50	5	3.69	6420	14410	33.9	38.1	0.45
50	5	3.69	6650	15140	35.1	40	0.44
60	1	3.64	33520	*86140*	35.8	46.1	0.39
60	5	3.64	9380	20900	50.2	55.9	0.45
60	1	3.64	32740	–	35	–	–
60	5	3.64	8180	20120	43.7	53.8	0.41
60	5	3.64	8210	19730	43.9	52.7	0.42
60	5	3.64	9250	22360	49.4	59.8	0.41
60	3	3.64	15800	31480	50.7	50.5	0.50
60	3	3.64	15010	29740	48.2	47.7	0.50
70	5	3.60	10690	26880	57.8	72.7	0.40
70	5	3.60	10080	26320	54.5	71.2	0.38
70	5	3.60	13520	28690	73.1	77.6	0.47
70	3	3.60	21600	40140	70.1	65.2	0.54
80	5	3.56	16070	–	88	–	–
80	5	3.56	16590	–	90.9	–	–
90	5	3.51	15710	–	87.1	–	–
90	10	3.51	12690	23380	140.7	129.6	0.54

activation energy for the BA dimer is close to the one measured for the methyl acrylate dimer via ESR [25] and via PLP–SEC [24], whereas the pre-exponential is above the one of the methyl acrylate dimer, which corresponds to the trend seen with the acrylate and methacrylate families. That the k_p value of butyl esters exceed the ones of the methyl ester may be explained by the better shielding of dipolar interactions by a butyl moiety.

In Table 2, Arrhenius parameters and bulk k_p at 25 °C for the methyl and butyl esters of the acrylate, methacrylate, and itaconate families are collated and compared to the ones of the associated acrylate dimers. In passing from the acrylates via the methacrylates to the itaconates, the pre-exponential, A, is strongly decreasing whereas the activation energy increases. The lowering of A is understood by the increase of the friction to internal rotation of the transition state structure. The accompanying increase in the activation energy may be due to an enhanced steric demand. Interestingly, the acrylate dimers do not fit into this series, as both activation energy and pre-exponential factor are above the values found for itaconates. The A values of the BA dimers even exceed the one reported for BMA. The additional methylene group in the acrylate dimers appears to be responsible for a reduced hindrance, as compared to the itaconates, of rotational motion in the transition state for propagation, which goes with an enhanced pre-exponential factor [40]. The relatively high activation energy of the acrylate dimers appears to reflect a significant steric hindrance in

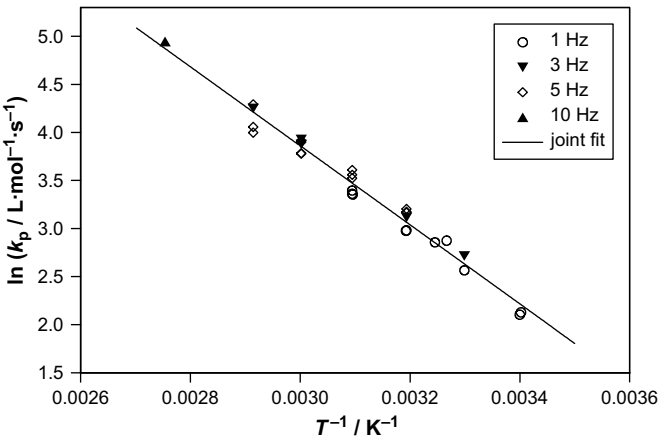

Fig. 2. Arrhenius plot of the k_p data from Table 1 for the temperature range 20–90 °C measured at various pulse repetition rates. The straight line depicts the best fit of the entire data set according to Eq. (2).

Table 2
Activation parameters and bulk propagation rate coefficients for 25 °C of the methyl and butyl members of the acrylate, methacrylate, itaconate, and acrylate dimer families. The monomer addition rate of midchain radicals in acrylate polymerization is also listed.

Monomer	A/L mol^{-1} s^{-1}	E_A/kJ mol^{-1}	$k_p^{25°C}$/L mol^{-1} s^{-1}	Ref.
MA	6.9×10^6	15.7	12250	[41]
BA	2.1×10^7	17.8	15980	[42]
MMA	2.7×10^6	22.4	320	[8]
n-BMA	3.8×10^6	22.9	370	[9]
DMI[a]	8.7×10^5	28.2	10.0	[12]
DnBI[a]	2.0×10^5	25.7	6.3	[12]
MA dimer	1.3×10^6	29.5	8.8	PLP, [24]
MA dimer	3.4×10^6	33.6	4.4	ESR, [25]
BA dimer	1.1×10^7	34.2	11.2	This work
BA-MCR	1.52×10^6	28.9	13.1	[29]

[a] Data from Ref. [12] with the Arrhenius parameters being deduced from the temperature range 0–20 °C in which depropagation appears to be negligible.

the transition state structure, which even slightly exceeds the one with itaconate propagation. The enhancement of both, E_A and A, in passing from itaconates to acrylate dimers results in fairly similar absolute k_p values for these two classes of monomers (see last column in Table 2).

Scheme 3 suggests that the propagation rate coefficient of butyl acrylate dimer and the monomer addition rate of midchain radicals in butyl acrylate homopolymerization should be close to each other. The respective rate coefficients at 25 °C are indeed relatively similar. On the other hand, the Arrhenius parameters do not perfectly agree. The difference in activation energy may be assigned to steric effects, as a significantly smaller molecule is added to the midchain radical as compared to the situation with BA dimer propagation. The activation energy of midchain radical propagation is however among the largest activation energies listed in Table 2, which indicates a similarity of BA dimer and BA-MCR propagation.

3.2. Termination rate coefficients from single pulse-pulsed laser polymerization experiments

For k_t determination via the SP-PLP–ESR method, the ESR spectrum of the propagating radical needs to be known. With respect to the immediate vicinity of the radical site, the radical species in BA dimer polymerization is similar to the midchain radical in butyl acrylate polymerization and should exhibit a similar ESR spectrum. Nine lines are observed (with two pairs of coinciding lines) for the BA midchain radical which has two slightly different $-CH_2-$ groups in the vicinity of the radical center [43,44]. Five lines can be identified for the BA dimer radical as shown in Fig. 3. They result from two pairs of protons both of virtually identical hyperfine splitting constants within the limits of spectral line broadening. The additional two protons in β-position to the radical site have no significant impact on the line splitting at the conditions under which the spectrum was taken. A spectrum consisting of five lines was also observed for the di-*n*-butyl itaconate radical [13,45].

In order to deduce $c_R(t)$ concentration vs time profiles from ESR data, a calibration of peak intensity at given magnetic field against radical concentration is required. Under properly selected experimental conditions, the double integral of the full ESR spectrum is directly proportional to the number of spins and hence to radical concentration [46]. Thus, the correlation between the double integral and the measured peak intensity of a particular ESR line needs to be precisely known. For various methacrylates [17,18] and for di-*n*-butyl itaconate [13] such linear correlations were observed. In contrast to this behavior, for the BA dimer, a lower than proportional increase of the total microwave absorbance is seen as a function of the line intensity at the ESR peak maximum (Fig. 4). This effect may result from line broadening upon increasing radical concentration. The correlation of the double integral with peak intensity may however be reasonably fitted by an arbitrary function. Calibration data from independent sets of experiments at

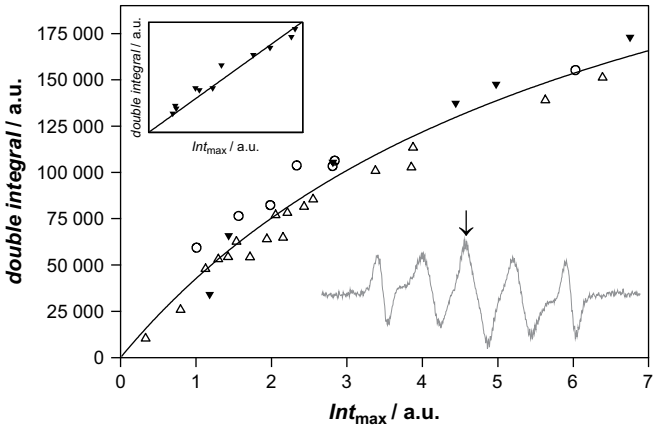

Fig. 4. Correlation between peak maximum intensity (at the position indicated by the arrow pointing to the spectrum) and double integral of the full ESR spectrum for various radical concentrations at −15 °C. The different symbols indicate independent experiments. The inset shows the associated correlation for +30 °C.

−15 °C are shown in Fig. 4 alongside with the fitted curve. The data for 0 °C also show such non-linear behavior. The curvature however becomes weaker toward increasing temperature and, within experimental accuracy, the data at 30 °C and above can be adequately fitted by a straight line as is shown in the inset to the figure.

Due to the non-linear calibration of the BA dimer radical spectrum at lower temperature, the analysis of time-resolved data is restricted to the determination of chain-length averaged $\langle k_t \rangle$, as the data treatment for deducing chain-length dependent k_t is highly sensitive toward the choice of the calibration fit function (A curvature of the correlation shown in Fig. 4 directly affects the radical decay vs time trace and thus $k_t(i)$, the variation of termination rate coefficient with chain length i.). The 30 °C data, however, could be analyzed with respect to chain-length dependent k_t, because double integral and peak intensity are linearly correlated at this temperature (see Fig. 4). The uncertainty in c_R is larger at high concentrations resulting from the non-linear calibration.

A $c_R(t)$ trace obtained for bulk BA dimer polymerization at 30 °C is depicted in Fig. 5. To improve signal to noise quality, 100 individual traces were co-added for this particular experiment. Compared to DnBI, BA dimer traces show a relatively fast decay in radical concentration, indicating that the termination rate coefficient is significantly larger, although both monomers are structurally similar and undergo relatively slow propagation. Thus, the increase in chain flexibility in passing from itaconates to acrylate dimers, which is indicated by the higher pre-exponential $A(k_p)$, appears to significantly affect also termination kinetics.

Chain-length-averaged termination rate coefficients have been obtained by fitting the time-resolved data to:

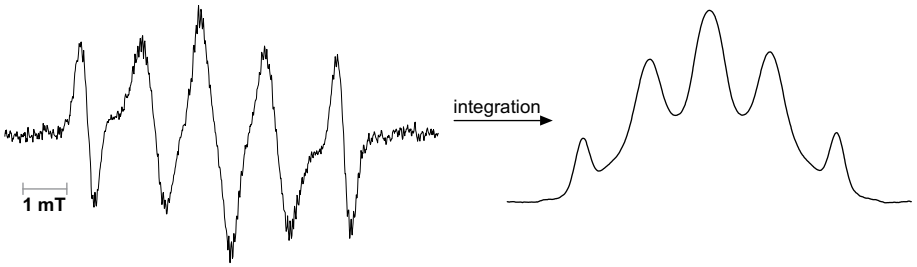

Fig. 3. l.h.s: ESR spectrum of the radical species in BA dimer polymerization at −15 °C under quasi-stationary reaction conditions and at a laser pulse repetition rate of 10 Hz (r.h.s: integral of the spectrum on the l.h.s).

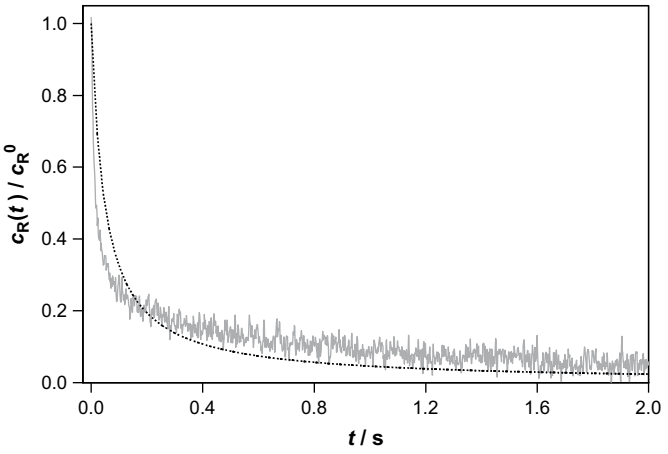

Fig. 5. Change in radical concentration after applying a laser pulse at $t = 0$ within a BA dimer free-radical polymerization at 30 °C and low degrees of monomer conversion as deduced via the SP–PLP–ESR. The signal results from co-adding 100 individual traces. The dotted line represents the best fit of the experimental data to Eq. (3).

$$\frac{c_R^0}{c_R(t)} = 1 + 2 \cdot \langle k_t \rangle \cdot c_R^0 \cdot t \qquad (3)$$

Fitting the $c_R(t)$ data to Eq. (3) results in the same type of deviation as observed with other monomers [13,17,18] thus indicating chain-length dependent k_t. Shortly after firing the laser pulse, experimental c_R decays at a higher rate than at times $t > 0.3$ s, where large radicals are present.

The traces have been fitted for the chain-length interval $1 < i < 10$, which is the largest one covered with all polymerization temperatures under investigation. At 30 °C the chain-length range could be measured even up to $i = 100$. No significant change in monomer conversion per pulse sequence occurs in these experiments where oligomeric rather than polymeric molecules are produced. The experiments were carried out exclusively at low levels of monomer consumption. Several experiments for deducing chain-length-averaged termination rate coefficients, $\langle k_t \rangle$, have been performed at each reaction condition. The arithmetic mean values

Table 3
Arrhenius parameters for the chain-length-averaged termination rate coefficient, $\langle k_t \rangle$, of several types of monomers each containing an *n*-butyl moiety.

Monomer	A/L mol^{-1} s^{-1}	E_A/kJ mol^{-1}	$k_t^{25°C}$/L mol^{-1} s^{-1}	Ref.
n-BMA[a]	2.1×10^{10}[a]	18.7	1.1×10^{7}[a]	[11]
DnBI	1.6×10^{9}	23.0	1.5×10^{5}	[13]
BA dimer	4.0×10^{10}	22.8	4.0×10^{6}	this work

[a] Values measured at 2000 bar and estimated for ambient pressure via the activation volume of $\langle k_t \rangle$ (13.8 cm^3 mol^{-1}) reported for BMA in [11].

of $\log\langle k_t \rangle$ are plotted as a function of polymerization temperature in Fig. 6. At 30 °C, $\langle k_t \rangle = 4.7 \times 10^6$ L mol^{-1} s^{-1} is found for the chain-length interval $1 < i < 10$. Fitting the data up to $i = 100$ yields 4×10^6 L mol^{-1} s^{-1} for $\langle k_t \rangle$.

Experiments at temperatures above 30 °C were not carried out in the present study, as termination rate would have become too fast to be accurately determined with the currently available time resolution of the SP-PLP–ESR set-up. The activation parameters of propagation and termination are, however, considered to be sufficiently accurate to allow for estimating rate coefficients for a more extended temperature range.

The error bars attached to the Arrhenius plot of $\langle k_t \rangle$ for the temperature range −15 to 30 °C (Fig. 6) indicate the standard deviations which result from averaging over several individual experiments. The Arrhenius parameters for the *n*-butyl dimer are $E_A(\langle k_t \rangle) = (22.8 \pm 3.7)$ kJ mol^{-1} and $\log(A/\text{L mol}^{-1}\,\text{s}^{-1}) = 10.6 \pm 1$. As can be seen from Table 3, the activation energy is thus close to $E_A(\langle k_t \rangle)$ of DnBI polymerization (23 kJ mol^{-1}) and to the experimental activation energies for average $\langle k_t \rangle$ in the initial period of *n*-butyl methacrylate (18.7 kJ mol^{-1}) and *tert*-butyl methacrylate (24.4 kJ mol^{-1}) bulk homopolymerizations [11]. The frequency factor, $A(\langle k_t \rangle)$ of DnBI ($\log(A/\text{L mol}^{-1}\,\text{s}^{-1}) = 9.2$) is however well below the one of the BA dimer value which suggests that the additional –CH_2– group in the dimer species provides higher chain mobility and/or less effective shielding of the radical functionality. The separation between the two ester groups of each monomeric unit is increased with the acrylate dimers. The brushes thus exhibit larger mobility and the polar interactions are diminished. The reduced stiffness of the polymer backbone

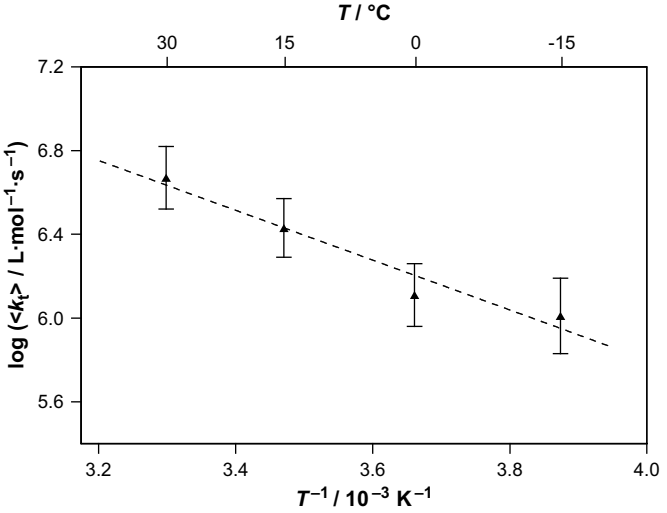

Fig. 6. Temperature dependence of $\langle k_t \rangle$ for BA dimer polymerization as deduced via the SP–PLP–ESR technique and by data-fitting for the time regime corresponding to the chain length range $1 < i < 10$ and to ideal polymerization kinetics (Eq. (3)). The error bars indicate the standard deviation from averaging over several individual experiments.

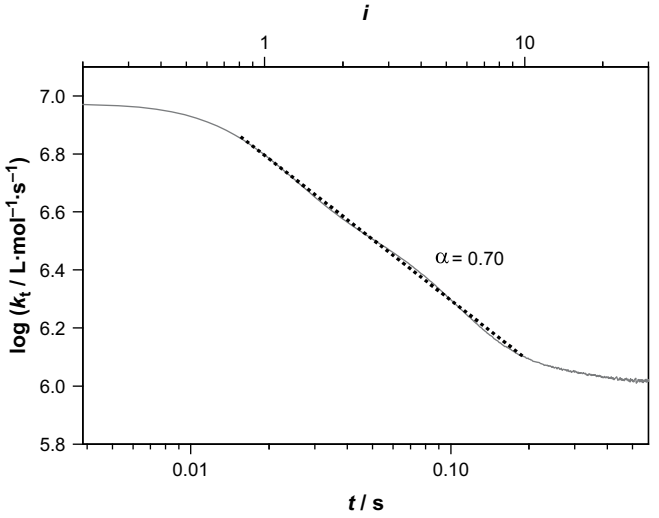

Fig. 7. Termination rate coefficient $k_t^{i,i}$ for two radicals of identical chain length i plotted as a function of time t after applying the laser pulse and of chain length i. The data is obtained via the "model free" approach (see text) for BA dimer polymerization at 30 °C. The dotted line represents power-law behavior of k_t with α being 0.7.

Table 4
Arrhenius parameters for the termination rate coefficient of two radicals of chain length unity, as deduced from pulsed laser experiments in conjunction with time-resolved ESR spectroscopic detection of radical concentrations.

Monomer	$\log[A(k_t^{1,1})/\mathrm{L\,mol^{-1}\,s^{-1}}]$	$E_A(k_t^{1,1})/\mathrm{kJ\,mol^{-1}}$	α_s	i_c	$\log[k_t^{1,1}(25\,^\circ\mathrm{C})/\mathrm{L\,mol^{-1}\,s^{-1}}]$	Ref.
n-BA[a]	10.1 ± 1.0	8.4 ± 2.5	0.85	30	8.6 ± 0.6	[47]
n-BMA	10.0 ± 1.0	10.1 ± 2.5	0.65	50	8.2 ± 0.6	[19]
DnBI	10.4 ± 1.0	27.6 ± 2.8	0.50	50	5.1 ± 0.8	[13]
BA dimer	10.9 ± 1.5	22.8 ± 4.0[b]	0.79	–	7.0 ± 0.6[c]	This work

[a] 1.52 M in toluene solution.
[b] Value measured for $\langle k_t \rangle$ (see Table 3) in the region of small chain lengths. The number should thus be close to $k_t^{1,1}$.
[c] Value refers to 30 °C.

enhances segmental diffusivity and thus $\langle k_t \rangle$ under conditions of segmental diffusion control which applies at low degrees of monomer conversion in methacrylate, itaconate and acrylate dimer bulk polymerizations. The $\langle k_t \rangle$ values for 25 °C in the last column of Table 3, which were estimated from the Arrhenius relations, are relatively similar for BMA and the BA dimer, whereas the associated number for DnBI is significantly lower, by almost two orders of magnitude. In Table 3, no comparison is made with the k_t data for butyl acrylate polymerization [5], as this would require the concentrations of secondary chain-end radicals and of MCRs to be precisely known, which is beyond the scope of the present article.

As the consequences of averaging over a population of radicals which differ in size or over a time interval in which radical size changes are not fully clear, it is recommendable to perform time-resolved measurements of radical concentration after applying a laser pulse, which is equivalent to measuring chain-length-dependent termination rate. The correlation of ESR peak maximum and double integral intensities, as has been mentioned above, is almost linear in case of BA dimer polymerization at 30 °C. Thus, the concentration vs time trace depicted in Fig. 5 may be analyzed for the chain-length dependency of k_t. The BA dimer radical is slowly propagating thus giving access to chain-length dependent k_t only at small chain lengths. The data is best analyzed by the so-called model-free approach [13], by which experimental $c_R(t)$ data are fitted to an arbitrary function (in the present case a sum of exponentials; $c_R(t)/c_R^0 = \sum_{n=1}^{5} A_n \exp(-t/B_n) + A_0$). The first derivative of the so-obtained expression is used to calculate k_t as a function of time without the interference of signal-to-noise, which usually prevents analysis of first-derivative values directly taken from primary experimental data. The function $k_t(t)$ is deduced from:

$$k_t(t) = -\frac{dc_R(t)}{dt} \cdot \left(2 \cdot c_R^2(t)\right)^{-1} \quad (4)$$

Fig. 7 depicts k_t as a function of time t after applying the laser pulse and thus as a function of chain length (see upper abscissa). The curve has been obtained by the model-free approach on the basis of the data in Fig. 5. The same procedure has already been applied to itaconate ESR data [13]. Almost constant k_t is found for the range of $0 < t < t_p = 0.019$ s that is in the region, where chain growth has not yet started (with $t_p = 1/(k_p c_M)$ being the time interval required for a single propagation step). The $k_t^{1,1}$ value in the initial plateau region is in excellent agreement with the value determined from fitting the experimental data to Eq. (3) in the same time interval: $k_t = 9.3 \cdot 10^6\,\mathrm{L\,mol^{-1}\,s^{-1}}$. From about $t = 0.019$ s on (that is where chain length exceeds $i = 1$), a steep decrease in the termination rate coefficient occurs up to chain length $i = 10$ at around 0.2 s. As is indicated by the straight line in Fig. 7, this decrease corresponds to a power-law exponent for short radicals of $\alpha_s = 0.7$ (where $k_t^{i,i} = k_t^0 i^{-\alpha}$). As the average value from several experiments at 30 °C, $\alpha_s = 0.79$ is obtained via the model-free approach.

The Arrhenius parameters for $k_t^{i,i}$ are listed in Table 4 together with the power-law exponents, α_s, which represent the chain-length dependence of $k_t^{i,i}$ at small chain lengths below i_c, the cross-over chain length. The activation energies, $E_A(k_t^{i,i})$, increase within the series BA, BMA, BA dimer, and DnBI. The $E_A(k_t^{i,i})$ value for BA dimer has been identified with the $E_A(\langle k_t \rangle)$ value deduced from the data plotted in Fig. 6. The activation energies for termination of both DnBI and BA dimer approach numbers as are typical for propagation steps. The pre-exponentials, $A(k_t^{i,i})$, are surprisingly similar for the four monomers (Table 4). The $A(k_t^{i,i})$ value for DnBI has been estimated from the activation energy, $E_A = 27.6 \pm 2.8\,\mathrm{kJ\,mol^{-1}}$ [13] and from $k_t^{i,i} = 2.5 \times 10^6\,\mathrm{L\,mol^{-1}\,s^{-1}}$ at 0 °C which value was calculated from the data at $i = 30$ and the $\alpha_s = 0.5$ (data point from Fig. 7 in Ref. [13]). The large differences in $k_t^{i,i}$ at the reference temperature of 25 °C (last column in Table 4) are predominantly due to differences in $E_A(k_t^{i,i})$.

The α_s value for the BA dimer, $\alpha_s = 0.79$, is above the numbers determined for BMA [19], $\alpha_s = 0.65$, and for di-butyl itaconate [13], $\alpha_s = 0.50$, but is fairly close to the value reported for BA polymerization in solution of toluene and is identical to α_s reported for methyl acrylate bulk polymerization [48]. The significant chain-length dependence of $k_t^{i,i}$ holds up to the cross-over chain length (see Table 4), which could not be determined for the BA dimer polymerization because of signal-to-noise quality becoming too poor toward higher chain lengths.

4. Conclusions

The BA dimer exhibits kinetic features of both di-butyl itaconate as well as butyl acrylate monomer. Steric factors appear to be responsible for the relatively large activation energies for propagation and termination, which are similar to the ones of di-*n*-butyl itaconate. The additional methylene group of BA dimer, on the other hand, induces similarity with the BA monomer, as is reflected by the relatively high frequency factors of the propagation and termination steps. Moreover, the short-chain-length dependence of the termination rate coefficient is similar for BA monomer and BA dimer. The low propagation rate coefficient of BA dimer in conjunction with the large termination rate coefficient results in the production of relatively low molecular weight BA dimer material, unless radical concentration is kept very small. Increasing temperature should be favorable for producing polymeric rather than oligomeric species, as propagation is associated with a slightly higher activation energy than is termination. Applying high pressure should have a stronger beneficial effect for producing high molecular weight material, as propagation is accelerated and termination is retarded.

Acknowledgements

T.J. is grateful to the *Deutsche Forschungsgemeinschaft* (DFG) for support during his Ph.D. thesis through the GRK 782 "Spectroscopy and Dynamics of Molecular Aggregates, Chains, and Coils". Additional financial support by the *Fonds der Chemischen Industrie* is

gratefully acknowledged. The authors also want to thank Robin Willemse and Alex van Herk for their support in determining Mark–Houwink coefficients for BA dimer.

References

[1] Olaj OF, Bitai I, Hinkelmann F. Makromol Chem 1987;188:1689–702.
[2] Buback M, Hippler H, Schweer J, Vögele HP. Makromol Chem Rapid Commun 1986;7:261–5.
[3] Buback M, Gilbert RG, Hutchinson RA, Klumperman B, Kuchta FD, Manders BG, et al. Macromol Chem Phys 1995;196:3267–80.
[4] Buback M, Kuchta FD. Macromol Chem Phys 1997;198:1455–80.
[5] Beuermann S, Buback M. Prog Polym Sci 2002;27:191–254.
[6] Asua JM, Beuermann S, Buback M, Castignolles P, Charleux B, Gilbert RG, et al. Macromol Chem Phys 2004;205:2151–60.
[7] Junkers T, Theis A, Davis TP, Buback M, Stenzel MH, Vana P, et al. Macromolecules 2005;38:9497–508.
[8] Beuermann S, Buback M, Davis TP, Gilbert RG, Hutchinson RA, Kajiwara A, et al. Macromol Chem Phys 2000;201:1355–64.
[9] Beuermann S, Buback M, Davis TP, Gilbert RG, Hutchinson RA, Olaj OF, et al. Macromol Chem Phys 1997;198:1545–60.
[10] Buback M, Kowollik C. Macromolecules 1998;31:3211–5.
[11] Buback M, Junkers T. Macromol Chem Phys 2006;207:1640–50.
[12] Szablan Z, Stenzel MH, Davis TP, Barner L, Barner-Kowollik C. Macromolecules 2005;38:5944–54.
[13] Buback M, Egorov M, Junkers T, Panchenko E. Macromol Chem Phys 2005;206:333–41.
[14] Hutchinson RA, Paquet DA, McMinn JH, Beuermann S, Fuller RE, Jackson EI. Dechema Monographs, vol. 131; 1995. p. 467.
[15] Junkers T, Voll D, Barner-Kowollik C. e-Polymers, in press.
[16] Barner-Kowollik C, Buback M, Egorov M, Fukuda T, Goto A, Olaj OF, et al. Prog Polym Sci 2005;30:605–43.
[17] Buback M, Egorov M, Junkers T, Panchenko E. Macromol Rapid Commun 2004;25:1004–9.
[18] Buback M, Müller E, Russell GT. J Phys Chem A 2006;110:3222–30.
[19] Barth J, Buback M, Hesse P, Sergeeva T. Macromolecules 2009;42:481–8.
[20] Szablan Z, Huaming M, Adler M, Stenzel MH, Davis TP, Barner-Kowollik C. J Polym Sci Part A Polym Chem 2007;45:1931–43.
[21] Chiefari J, Jeffery J, Mayadunne RTA, Moad G, Rizzardo E, Thang SH. Macromolecules 1999;32:7700–4.
[22] Junkers T, Bennet F, Koo SPS, Barner-Kowollik C. J Polym Sci Part A Polym Chem 2008;46:3433–7.
[23] Hirano T, Zetterlund PB, Yamada B. Polym J 2003;35:491–500.
[24] Tanaka K, Yamada B, Fellows CM, Gilbert RG, Davis TP, Yee LH, et al. J Polym Sci Part A Polym Chem 2001;39:3902–15.
[25] Kobatake S, Yamada B. J Polym Sci Part A Polym Chem 1996;34:95–108.
[26] Kobatake S, Yamada B. Macromol Chem Phys 2003;198:2825–37.
[27] Junkers T, Barner-Kowollik C. J Polym Sci Part A Polym Chem 2008;46:7585–605.
[28] Koo SPS, Junkers T, Barner-Kowollik C. Macromolecules 2009;42:62–9.
[29] Nikitin AN, Hutchinson RA, Buback M, Hesse P. Macromolecules 2007; 40:8631–41.
[30] Britton D, Heatley F, Lovell PA. Macromolecules 1998;31:2828–37.
[31] Buback M. Angew Chem 1991;103:641–53.
[32] Müller M. Ph.D. Thesis, Göttingen; 2005.
[33] Strazielle C, Benoit H, Vogl O. Eur Polym J 1978;14:331–4.
[34] Buback M, Kuelpmann A. Maromol Chem Phys 2003;204:632–7.
[35] Vana P, Davis TP, Barner-Kowollik C. Aust J Chem 2002;55:315–8.
[36] Buback M, Egorov M, Feldermann A. Macromolecules 2004;37:1768–76.
[37] Olaj OF, Zoder M, Vana P, Kornherr A, Schnoll-Bitai I, Zifferer G. Macromolecules 2005;38:1944–8.
[38] Heuts JPA, Russell GT. Eur Polym J 2006;42:3–20.
[39] Heuts JPA, Russell GT, Smith GB, van Herk AM. Macromol Symp 2007; 248:12–22.
[40] Beuermann S, Buback M, Hesse P, Lacik I. Macromolecules 2006;39:184–93.
[41] Buback M, Kurz CH, Schmaltz C. Macromol Chem Phys 1998;199:1721–7.
[42] Barner-Kowollik C, Günzler F, Junkers T. Macromolecules 2008;41:8971–3.
[43] Willemse RXE, van Herk A, Panchenko E, Junkers T, Buback M. Macromolecules 2005;38:5098–103.
[44] Buback M, Hesse P, Junkers T, Sergeeva T, Theis T. Macromolecules 2008;41:288–91.
[45] Otsu T, Yamagishi K, Yoshioka M. Macromolecules 1992;25:2713–6.
[46] Kamachi M. J Polym Sci Part A Polym Chem 2002;40:269–85.
[47] Hesse P. Ph.D. Thesis, Universität Göttingen, ISBN 978-3-86727-682-5.
[48] Buback M, Hesse P, Junkers T, Theis T, Vana P. Aust J Chem 2007;60:779–87.